CFSRC COLLOQUIUM

*Proceedings of the Cold-Formed Steel Research Consortium Colloquium*
*20-22 October 2020 (cfsrc.org)*

# Experimental Study on the High Temperature Properties of Advanced High-Strength Cold-formed Steels

Xia Yan[1], Yu Xia[2], Hannah B. Blum[2], Thomas Gernay[1]

## Abstract

Recent advances in steel manufacturing have led to materials with greatly enhanced capabilities at competitive cost. New types of steel, referred to as Advanced High-Strength Steels (AHSS), have been developed for automotive applications with yield strengths up to 1200 MPa, ultimate strengths up to 1900 MPa, and relatively large tensile elongations. Efficiently harnessed, the adoption of AHSS materials in the construction industry can provide many benefits, notably with cold-formed steel structures which provide efficient, lightweight, and resilient solutions for a range of building applications. However, the behavior of these novel materials still needs to be characterized under extreme environments which may arise in structural applications, including high temperatures resulting from fire. To fill this gap, an experimental investigation was carried out on the mechanical properties at elevated temperature and after cooling down of six different steel grades. The tested materials included dual-phase steel (DP), martensitic steel (MS), and high-strength low-alloy steel (HSLA) with nominal yield strengths ranging from 340 to 1200 MPa and nominal ultimate strengths ranging from 480 to 1500 MPa. Three types of high temperature regimes, namely steady-state, transient-state, and residual tests, were applied at temperatures up to 700°C. Material properties were obtained including elastic modulus, yield stress, and ultimate stress. The test results were compared with the prediction models in Eurocode 3 and AISC 360, and other published test data. Comparisons showed that AHSS steels exhibit larger reduction in stiffness and strength than lower grade cold-formed steels at elevated temperature and after cooling down.

## 1. Introduction

There has been an increasing demand for high performance steels in the construction industry. Advanced high-strength steels (AHSS) with nominal yield stress up to 1200 MPa are now available in the market and have been widely used in the automotive industry [1]. Given their improved combination of strength and ductility, AHSS steels show great potential to be used as next-generation materials in structural applications. The adoption of AHSS can further reduce the dimension of structural components, overall weight, and transportation costs, and provide enhanced structural safety and resilience [2].

AHSS refers to a group of steels that feature multiphase microstructure resulting from precise heating and cooling procedure from the austenite or austenite/ferrite phase [3]. Therefore, AHSS contains one or more phases, such as martensite, austenite, or bainite, other than ferrite, pearlite, or cementite phase. AHSS include dual phase (DP), ferritic-bainitic (FB), martensitic (MS) and other complex-phase steels. AHSS can be hot-rolled or cold-formed. Compared with conventional low- and high-strength steels that have single-phase microstructure, AHSS exhibit a wide range of strength, ductility, toughness, and fatigue properties.

A sound knowledge of the performance of any new materials under different working conditions is fundamental for design practice for civil engineers. Fire is one of the extreme conditions that may arise and lead to the degradation of mechanical properties of the materials [4]. Thus, characterization of the performance of AHSS at elevated temperature and after cooling down is crucial for the structural fire safety design. However, design provisions in current standards and codes, such as Eurocode 3 [5] and AISC [6], are mainly based on hot-rolled steels and of normal grades. The cold working that increases the strength of the steels may be lost quickly at elevated temperature. This effect can be even more pronounced for high-strength cold-formed steels, while other effects can also be at play for multiphase AHSS when exposed to high temperature.

[1] Johns Hopkins University, Baltimore, MD, USA
[2] University of Wisconsin-Madison, Madison, WI, USA

Research on the mechanical properties of conventional cold-formed high-strength steel at elevated temperature and after cooling down can be found in some published papers. For the elevated temperature mechanical properties, Lee et al. [7] tested cold-formed G500 and G550, Chen and Young [8] investigated cold-formed G450 and G550, and Li and Young [9] tested cold-formed steels with nominal yield stress of 700 MPa and 900 MPa. They compared their tested results with the predictions in design standards. As for the post-fire mechanical properties, Gunalan and Mahendran [10] tested cold-formed G500 and G550, Li and Young [11] tested cold-formed steels with nominal yield stress of 700 MPa and 900 MPa, and Chen et al. [12] tested cold-formed G550. Overall, the test data from these studies reveal that the retention factors provided in current design codes on the basis of hot-rolled steels are not suitable to predict the performance of cold-formed steel at elevated temperature nor after cooling down. Meanwhile, test data on advanced high-strength steels with nominal yield stress up to 1200 MPa remains very limited.

To fill this gap, this study presents an experimental investigation to characterize the elevated temperature and post-fire mechanical properties of four AHSS steels in addition to one conventional mild steel and one HSLA steel used as benchmarks [3,13]. Tensile specimens were cut from cold-formed steel sheets and tested in three different regimes, namely steady-state test, transient-state test, and residual test. Mechanical properties including elastic modulus, yield stress, and ultimate stress were extracted from the obtained stress-strain curves. The reduction of the mechanical properties of the tested materials, in terms of retention factors, are compared with the predictive models in design codes and other literature data.

## 2. Experimental study

### *2.1 Materials and specimens*

Six steel materials are investigated in this study including four AHSS steels and two conventional steels. The four AHSS steels include two dual-phase (DP) steels and two martensitic (MS) steels. The microstructure of DP steel is a mixture of soft ferritic matrix and discreet martensitic islands as the second phase. It features a good balance of strength and ductility and high ultimate to yield stress ratio, which is good for energy absorption. MS steel is best known for its extremely high strength and is rich in martensitic matrix containing a small amount of ferritic and bainitic phase. It is typically produced by quenching at a very fast rate following hot-rolling, annealing, or a post-forming heat treatment. The two conventional steels include a mild steel and a high-strength low-alloy (HSLA) steel. Naming of the specimens is based on the microstructure and nominal yield stress, namely Mild-395, HSLA-700, DP-340, DP-700, MS-1030, and MS-1200. The nominal strength and nominal thickness of each steel type are listed in Table 1.

The specimens were cut in the longitudinal direction of the steel sheets. The shape and dimension of the specimens were prepared in accordance with ASTM E21 [14] and ASTM E8 [15] for pin-loaded tensile testing of metallic materials with 12.7mm (0.5 in) width and 50 mm (2 in) gauge length of the reduced parallel section, as shown in Figure 1. The specimens were cut by waterjet and then milling was applied for accuracy. Measurement of the practical thickness of width of each specimen was carried out at the two ends and center of the reduced parallel section. The average value was used to calculate the mechanical properties. For coated specimens, the coating was removed by acid and the average zinc coating thickness was found to be 0.04 mm. The coating thickness was subtracted from the measured thickness.

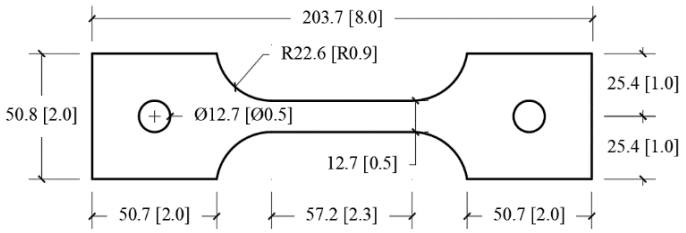


Figure 1: Shape and dimension of the specimen (unit in mm and inch).

Table 1: Nominal strength and nominal thickness of the tested steels.

| Steel type | $f_{y,20}$ (MPa) | $f_{u,20}$ (MPa) | Thickness (mm) | Coating |
|---|---|---|---|---|
| Mild-395 | 395 | 482 | 1.4 | Coated |
| HSLA-700 | 700 | 980 | 0.6 | Coated |
| DP-340 | 340 | 590 | 1.4 | Uncoated |
| DP-700 | 700 | 980 | 1.4 | Coated |
| MS-1030 | 1030 | 1300 | 1.0 | Uncoated |
| MS-1200 | 1200 | 1500 | 1.0 | Uncoated |

### *2.2 Test set-up*

An ATS high temperature furnace with three independent heating zones was used to heat up the specimens. The furnace was controlled by an ATS control system which can set up the target temperature and heating rate. Tensile force was applied by an MTS loading frame. During heating, the steel surface temperature was measured by three external thermocouples which were located at the two ends and the center of the reduced parallel section. The strain was measured by both a high temperature extensometer (-10%/20%) and digital image correlation (DIC) method. A specifically developed LabVIEW program was used to control the loading process and record the test data.

*2.3 Test procedure*

Three different tests were carried out in this study, namely steady-state test, transient-sate test, and residual test. To study the mechanical properties of AHSS steels at elevated temperature, steady-state tests were conducted on all the six materials (conventional steels as benchmark), and transient-state tests were conducted on DP-700 and MS-1200. Residual tests were conducted on the four AHSS steels to investigate the post-fire performance.

In steady-state test, the specimens were heated to elevated temperatures up to 700°C with a heating rate of 10°C/min. After the target temperature was reached, an extra 15-20 minutes of heating was maintained to ensure the uniform temperature inside the specimen. After that, tensile force was applied to the specimen with a loading rate of 0.25mm/min until fracture, while the temperature was maintained constant. In transient-state test, the specimens were first loaded in tension to target stress levels and then heated at a rate of 5°C/min until fracture, while the force was maintained constant. In residual test, the specimens were heated to elevated temperatures up to 700°C with a heating rate of 25°C/min while unloaded. An extra 20 minutes of heating was maintained to ensure the uniform temperature inside the specimen. After that, the specimens were taken out of the furnace and cooled down to ambient temperature in the air. Tensile tests were then carried out on the specimen at ambient temperature to obtain the post-fire mechanical properties.

*2.4 Definition of mechanical properties*

During the test, the applied force was output from the load cell, and the strain was measured from both extensometer and DIC method. As long as the strain was smaller than 20%, the results from the extensometer were used. Once the strain exceeded 20%, the DIC results were used.

The elastic modulus $E$, 0.2% proof stress $f_{0.2}$, and 2.0% stress $f_{2.0}$, and ultimate stress $f_u$ were extracted from the obtained stress-strain curves. The elastic modulus was obtained as the initial slope of the stress-strain curve following the method in [3]. The 0.2% proof stress is the stress needed to impart 0.2% plastic strain. The ultimate stress is the maximum stress measured during loading.

The reduction trend of mechanical properties with increasing temperature or exposure temperature is described by the definition of retention factors in this study. For steady-state tests and transient-state tests, the retention factors are determined as the ratio of the mechanical properties at elevated temperature to their original values at ambient temperature. For residual tests, the retention factors are determined as the ratio of the mechanical properties after exposure to elevated temperature to their original values at ambient temperature. The retention factors are noted as $k_E$ for elastic modulus, $k_{0.2}$ for the 0.2% proof stress, $k_{2.0}$ for the stress at 2.0% strain, and $k_u$ for the ultimate stress.

## 3. Test results

*3.1 Steady-state tests*

The stress-strain curves obtained from the steady-state tests are plotted in Figure 2. The overall trend of reducing stiffness and strength of steels with increasing temperature can be observed. The measured mechanical properties including elastic modulus, 0.2% proof stress, stress at 2.0% strain, and ultimate stress are listed in Table 2 to Table 5.

Table 2: Elastic modulus $E$ obtained from steady-state tests.

| T (°C) | E (GPa) | | | | | |
|---|---|---|---|---|---|---|
| | Mild-395 | HSLA-700 | DP-340 | DP-700 | MS-1030 | MS-1200 |
| 20 | 213.0 | 218.0 | 210.0 | 209.8 | 215.6 | 208.6 |
| 200 | 182.7 | 180.2 | 174.3 | 176.6 | 218.6 | 177.9 |
| 300 | 159.8 | 166.6 | 152.6 | 155.6 | 172.8 | 152.4 |
| 400 | 139.6 | 143.6 | 134.9 | 147.8 | 117.1 | 112.7 |
| 500 | 116.9 | 91.7 | 115.6 | 106.1 | 60.3 | 66.7 |
| 600 | 91.5 | 67.5 | 98.8 | 68.4 | 40.0 | 37.6 |
| 700 | 60.4 | 49.1 | 75.1 | 47.1 | 19.9 | 18.7 |

Table 3: 0.2% proof stress $f_{0.2}$ obtained from steady-state tests.

| T (°C) | $f_{0.2}$ (MPa) | | | | | |
|---|---|---|---|---|---|---|
| | Mild-395 | HSLA-700 | DP-340 | DP-700 | MS-1030 | MS-1200 |
| 20 | 393 | 752 | 424 | 762 | 1327 | 1387 |
| 200 | 355 | 739 | 430 | 740 | 1128 | 1222 |
| 300 | 349 | 740 | 359 | 671 | 925 | 887 |
| 400 | 292 | 608 | 276 | 495 | 549 | 506 |
| 500 | 209 | 363 | 171 | 262 | 228 | 223 |
| 600 | 108 | 120 | 97 | 112 | 95 | 78 |
| 700 | 51 | 30 | 41 | 42 | 26 | 28 |

Table 4: Stress at 2.0% strain $f_{2.0}$ obtained from steady-state tests.

| T (°C) | $f_{2.0}$ (MPa) | | | | | |
|---|---|---|---|---|---|---|
| | Mild-395 | HSLA-700 | DP-340 | DP-700 | MS-1030 | MS-1200 |
| 20 | 411 | 1013 | 542 | 971 | 1418 | 1572 |
| 200 | 414 | 969 | 608 | 996 | 1440 | 1524 |
| 300 | 414 | 968 | 507 | 887 | 1035 | 1066 |
| 400 | 333 | 743 | 338 | 588 | 568 | 566 |
| 500 | 227 | 421 | 190 | 302 | 266 | 273 |
| 600 | 112 | 137 | 101 | 120 | 111 | 95 |
| 700 | 53 | 38 | 44 | 50 | 34 | 36 |

Table 5: Ultimate stress $f_u$ obtained from steady-state tests.

| T (°C) | $f_u$ (MPa) | | | | | |
|---|---|---|---|---|---|---|
| | Mild-395 | HSLA-700 | DP-340 | DP-700 | MS-1030 | MS-1200 |
| 20 | 486 | 1106 | 675 | 1026 | 1428 | 1608 |
| 200 | 493 | 1045 | 772 | 1099 | 1509 | 1618 |
| 300 | 513 | 1079 | 620 | 983 | 1038 | 1069 |
| 400 | 365 | 769 | 357 | 591 | 578 | 569 |
| 500 | 235 | 426 | 194 | 306 | 271 | 278 |
| 600 | 115 | 141 | 103 | 124 | 114 | 99 |
| 700 | 54 | 43 | 45 | 51 | 43 | 43 |

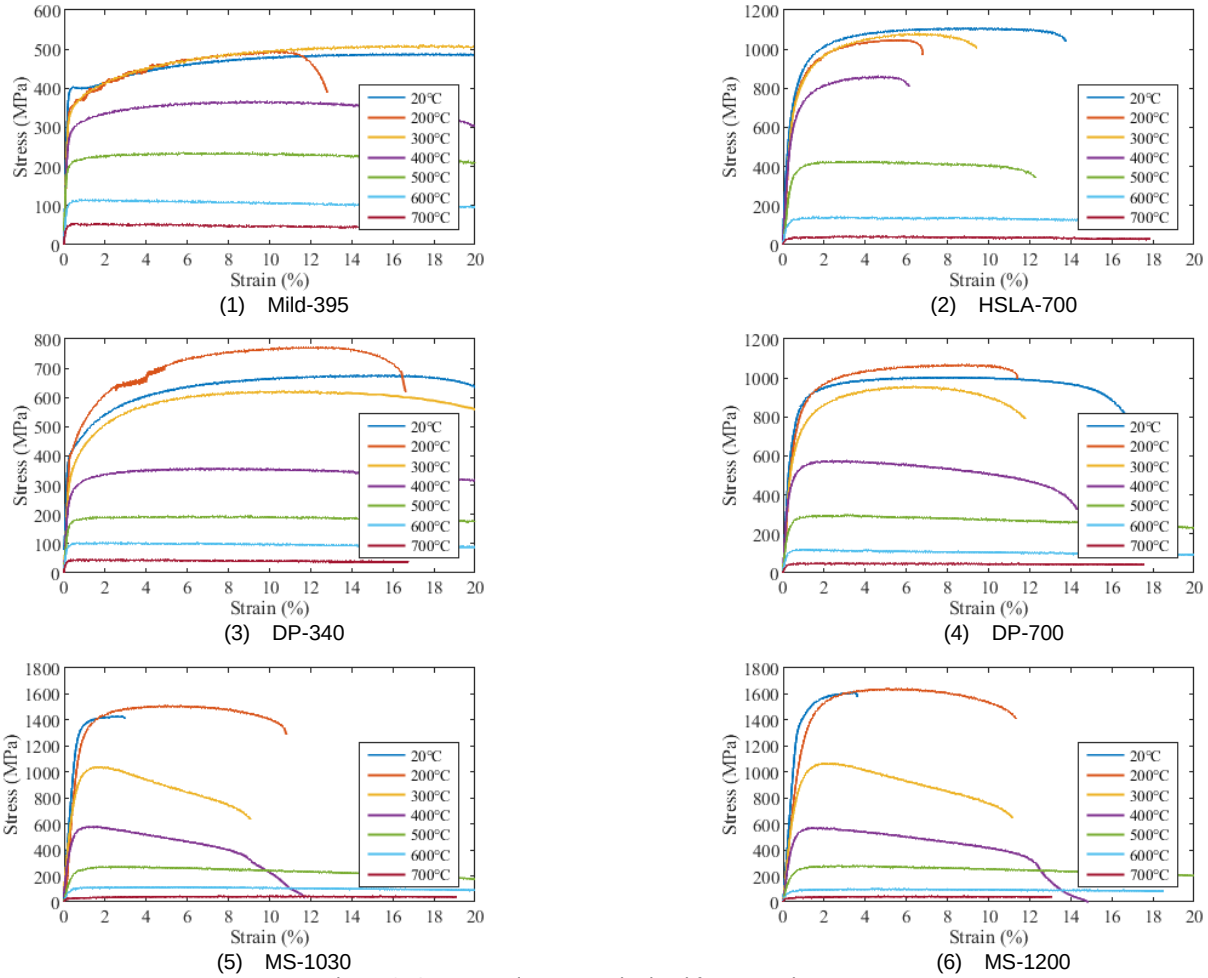


(1) Mild-395 (2) HSLA-700

(3) DP-340 (4) DP-700

(5) MS-1030 (6) MS-1200

Figure 2: Stress-strain curves obtained from steady-state tests.

*3.2 Transient-state tests*

In transient-state test, the measured strain under a given stress state at elevated temperature is the sum of thermal strain and mechanical strain. To obtain the mechanical strain, zero-load tests were carried out to measure the free thermal strain. By subtracting the thermal strain from the total strain, the relationship between mechanical strain and the temperature was obtained under different stress states. The full set of temperature-mechanical strain curves were converted into stress-strain curves at different temperatures. Since the tested stress levels are limited, the stress-strain curves are described by a number of discrete points, as shown in Figure 3. Mechanical properties obtained from transient-state tests are listed in Table 6 and Table 7.

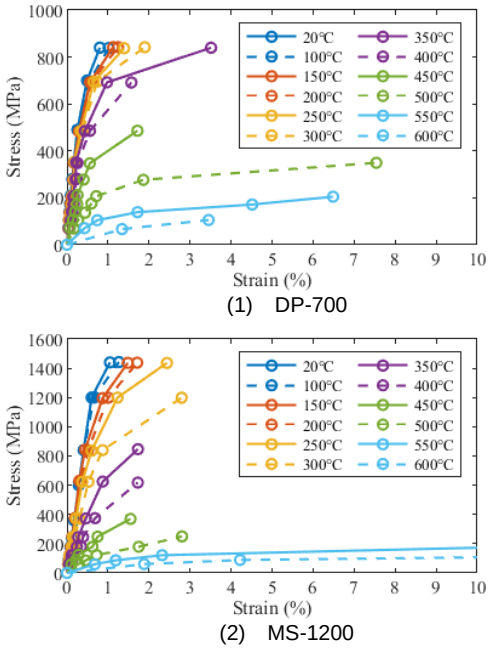


(1) DP-700

(2) MS-1200

Figure 3: Stress-strain curves obtained from transient-state tests.

Table 6: Elastic modulus $E$ obtained from transient-state tests.

| T (°C) | E (GPa) | |
|---|---|---|
| | DP-700 | MS-1200 |
| 100 | 184.1 | 227.7 |
| 150 | 168.8 | 217.4 |
| 200 | 158.2 | 197.7 |
| 250 | 160.5 | 183.3 |
| 300 | 158.7 | 118.6 |
| 350 | 151.5 | 75.7 |
| 400 | 133.4 | 48.0 |
| 450 | 55.0 | 37.0 |
| 500 | 41.3 | 20.5 |
| 550 | 16.6 | 8.8 |
| 600 | 5.0 | 3.2 |

Table 7: Yield stresses obtained from transient-state tests.

| T (°C) | $f_{0.2}$ (MPa) | | $f_{2.0}$ (MPa) | |
|---|---|---|---|---|
| | DP-700 | MS-1200 | DP-700 | MS-1200 |
| 100 | 707 | 1233 | - | - |
| 150 | 707 | 1034 | - | - |
| 200 | 706 | 965 | - | - |
| 250 | 671 | 879 | - | 1350 |
| 300 | 602 | 847 | - | 1050 |
| 350 | 527 | 684 | 752 | - |
| 400 | 483 | 508 | - | - |
| 450 | 388 | 279 | - | - |
| 500 | 198 | 128 | 279 | 196 |
| 550 | 109 | 84 | 143 | 111 |
| 600 | 73 | 65 | 79 | 62 |

### *3.3 Residual tests*

The stress-strain curves from residual tests are shown in Figure 4 and the properties are listed in Table 8 to Table 11.

Table 8: Elastic modulus obtained from residual tests.

| T (°C) | E (GPa) | | | |
|---|---|---|---|---|
| | DP-340 | DP-700 | MS-1030 | MS-1200 |
| 200 | 212.5 | 208.1 | 212.3 | 203.3 |
| 300 | 191.9 | 213.9 | 219.9 | 210.4 |
| 400 | 218.7 | 210.9 | 210.1 | 204.8 |
| 500 | 206.5 | 225.1 | 218.6 | 228.3 |
| 600 | 206.4 | 218.3 | 232.1 | 211.9 |
| 700 | 195.2 | 163.3 | 196.8 | 189.0 |

Table 9: 0.2% proof stress $f_{0.2}$ obtained from residual tests.

| T (°C) | $f_{0.2}$ (MPa) | | | |
|---|---|---|---|---|
| | DP-340 | DP-700 | MS-1030 | MS-1200 |
| 200 | 527 | 803 | 1403 | 1413 |
| 300 | 499 | 890 | 1371 | 1374 |
| 400 | 491 | 791 | 1030 | 1105 |
| 500 | 434 | 627 | 752 | 838 |
| 600 | 382 | 454 | 654 | 710 |
| 700 | 354 | 358 | 423 | 492 |

Table 10: Stress at 2.0% strain $f_{2.0}$ obtained from residual tests.

| T (°C) | $f_{2.0}$ (MPa) | | | |
|---|---|---|---|---|
| | DP-340 | DP-700 | MS-1030 | MS-1200 |
| 200 | 548 | 962 | 1445 | 1558 |
| 300 | 535 | 934 | 1381 | 1418 |
| 400 | 488 | 826 | 1036 | 1106 |
| 500 | 432 | 632 | 751 | 838 |
| 600 | 383 | 462 | 658 | 703 |
| 700 | 354 | 552 | 429 | 482 |

Table 11: Ultimate stress $f_u$ obtained from residual tests.

| T (°C) | $f_u$ (MPa) | | | |
|---|---|---|---|---|
| | DP-340 | DP-700 | MS-1030 | MS-1200 |
| 200 | 691 | 1011 | 1456 | 1596 |
| 300 | 649 | 983 | 1390 | 1438 |
| 400 | 579 | 874 | 1041 | 1134 |
| 500 | 509 | 702 | 783 | 860 |
| 600 | 460 | 550 | 673 | 769 |
| 700 | 449 | 715 | 482 | 516 |

## 4. Discussions

### *4.1 Elastic modulus*

The retention factors of elastic modulus, $k_E$, are plotted in Figure 5. For DP-700, the transient-state tests yield similar results with steady-state tests for temperatures up to 400°C, beyond which transient-state tests yield lower elastic modulus. For MS-1200, the two test methods yield similar results for temperature up to 300°C, beyond which a larger discrepancy can be observed. This may be due to the thermal creep effect which becomes more noticeable when the temperature is higher than one third of the melting temperature of the materials. The test results are also compared with the prediction in Eurocode 3 [5] and AISC-360 [6]. Generally, the retention factors given by the design codes are suitable to predict the performance of Mild-395 and DP-400, but unconservative for HSLA-700, DP-700, and the two tested MS steels. Besides, the comparisons to previously published data show that the tested AHSS steels show larger reduction in elastic modulus at elevated temperature than other conventional steels. The G550 from Lee et al. [7] show similar reduction trend as the DP-700 steel in this study but are not conservative for the MS steels.

The post-fire (residual) retention factors for the modulus are shown in Figure 6. The tested AHSS steels maintain their elastic modulus after exposure to temperature up to 600°C, while a permanent reduction can be observed after exposure to 700°C. The test results align well with other literature data. The test results are also compared with the prediction of elastic modulus at elevated temperature. It is clear that the retention factors at elevated temperature given by EC3 [5] are not applicable to predict the post-fire elastic modulus of the tested AHSS steels, since the modulus is largely recoverable.

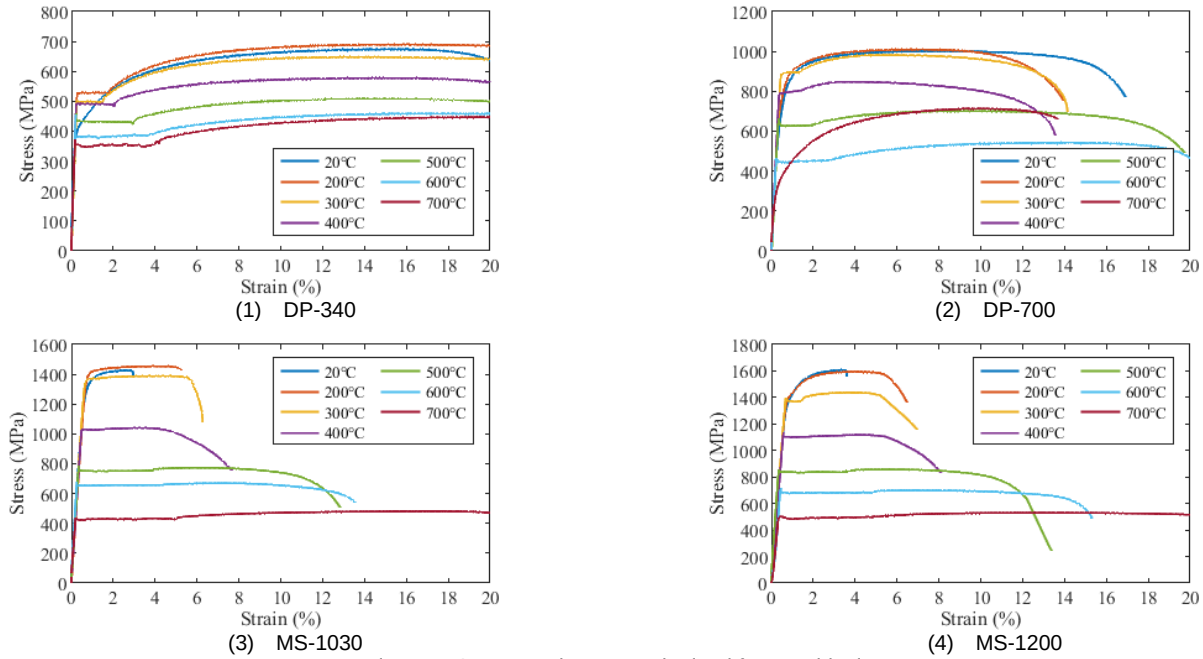


(1) DP-340 (2) DP-700

(3) MS-1030 (4) MS-1200

Figure 4: Stress-strain curves obtained from residual tests.

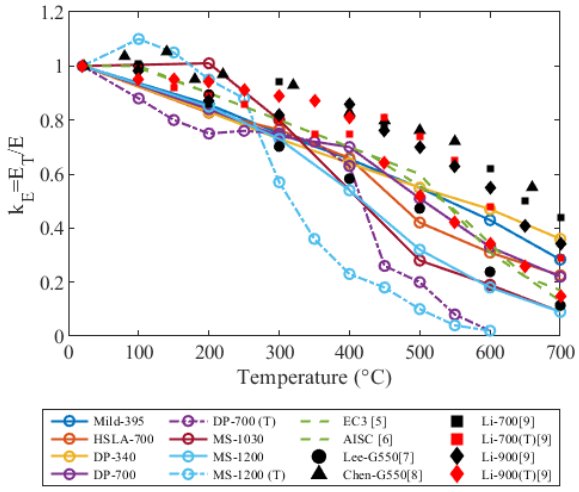


Figure 5: Comparison of elastic modulus obtained from steady-state tests and transient-state tests (marked with 'T').

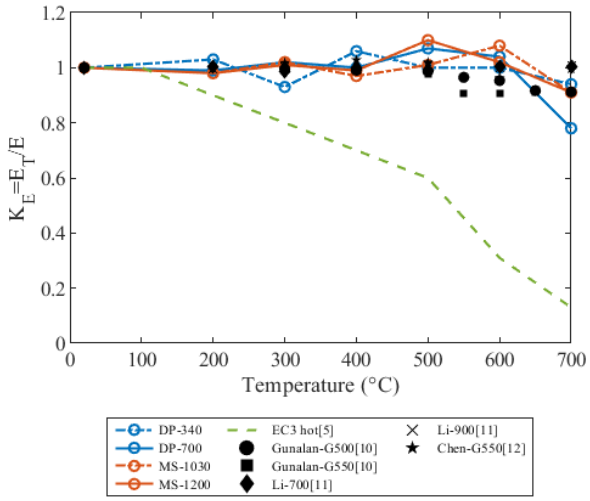


Figure 6: Comparison of elastic modulus obtained from residual tests. The EC3 value is at elevated temperature.

*4.2 Yield stress*

The retention factors of the 0.2% proof stress obtained from the steady-state tests and transient-state tests are shown in Figure 7. The yield stress of the tested AHSS steels reduces markedly when the temperature is higher than 300°C. At 700°C, DP-700 maintains about 5% of its original 0.2% proof stress at ambient temperature, while the two MS steels maintain 2% of their ambient temperature 0.2% proof stress. When comparing the yield stresses obtained from the two test methods, unlike with the elastic modulus, there is no significant influence of the testing method on the yield stresses. The test results are also compared with the predictions given by Eurocode 3 [5] on cold-formed class 4 sections and other literature data. The prediction given by EC3 [5] is suitable to predict the yield stress of Mild-395, but unconservative for the tested HSLA-700 and AHSS steels. The G550 tested by Chen and Young [8] lie within the range of the results in this study. However, the tested AHSS generally show larger reduction in yield stress than the other literature data, which suggests that the cold-formed AHSS are more affected by the elevated temperature.

The residual 0.2% proof stress of the tested materials after exposure to elevated temperature is shown in Figure 8. The two MS steels show quite similar trend, while DP-700 shows larger reduction in yield stress than DP-340. The test results are also compared with the retention factors of 0.2% proof stress given by EC3 [5] at elevated temperature and other literature data. The EC3 values at elevated temperature [5], shown for reference, lie beneath the post-fire data of AHSS. The data on the DP-340 in this study aligns well with other conventional steel data from the literature. The DP-700, MS-1030, and MS-1200 show larger reduction in yield stress in temperature range of 300°C~500°C, but show similar results with the G500 and G550 tested by Gunalan and Mahendran [10] at 600°C and 700°C.

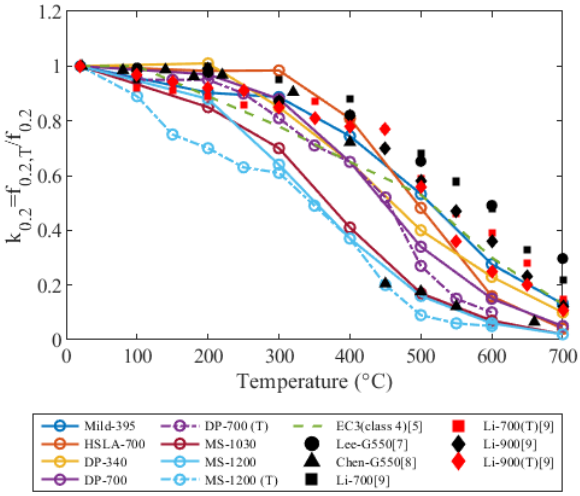


Figure 7: Comparison of 0.2% proof stress obtained from steady-state tests and transient-state tests (marked with 'T').

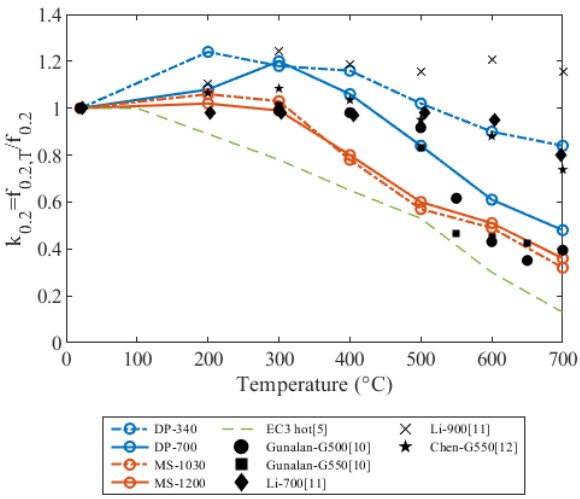


Figure 8: Comparison of 0.2% proof stress obtained from residual tests. The EC3 value is at elevated temperature.

*4.3 Ultimate stress*

The retention factors of the ultimate stress are plotted in Figure 9. The Mild-395, HSLA-700, DP-340, and DP-700 start to lose their original ultimate stress at temperature higher than 400°C, while the two MS steels start to lose their original ultimate stress at temperature higher than 300°C. The prediction of ultimate stress at elevated temperature given by EC3 [5] and AISC-360 [6] are unconservative to predict the ultimate stress of the tested materials. The G550 tested by Chen and Young [8] show similar results with the AHSS in this study, but the 700 and 900 steel tested by Li and Young [9] show higher retention factors in ultimate stress than the tested materials in this study.

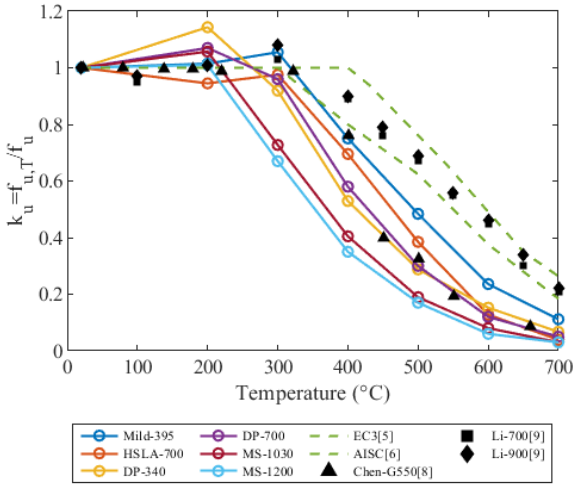


Figure 9: Comparison of ultimate stress obtained from steady-state tests.

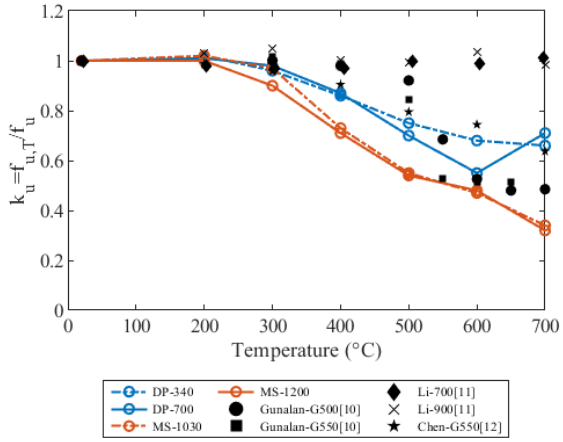


Figure 10: Comparison of ultimate stress obtained from residual tests.

The residual ultimate stress is shown in Figure 10. The two MS steels show similar results. The ultimate stress of the DP-700 exhibits a rebound at 700°C. Comparisons with other literature data show that the retention factors of ultimate stress of the two DP steels lie within other literature data, while the two MS steels show larger reduction in ultimate stress than the other conventional steels.

## 5. Conclusions

An experimental investigation has been carried out on the mechanical properties of advanced high-strength steels (AHSS) at elevated temperature and after exposure to elevated temperature. Six steel types were investigated including one conventional mild steel Mild-395, one high-strength low-alloy steel HSLA-700, and four AHSS steels, namely DP-340, DP-700, MS-1030, and MS-1200. Stress-strain curves as well as mechanical properties were reported. Reduction trends of the mechanical properties in terms of retention factors with increasing temperature or exposure temperature were discussed and compared with predictions in deign codes and other literature data. The following conclusions can be drawn:

- The mechanical properties of the tested cold-formed AHSS are greatly influenced by the elevated temperature as well as exposure temperature.

- The cold-formed AHSS materials tested in this study experience larger reduction of properties at elevated temperature than conventional cold-formed steels. They also experience larger permanent reduction (post-fire), and starting at a lower exposure temperature, compared with conventional cold-formed steels. Therefore, these AHSS materials exhibit a distinct high temperature response which warrant specific study and provisions.

- The retention factors at elevated temperature given in Eurocode 3 [5] for elastic modulus, 0.2% proof stress, and ultimate stress are adequate for the tested Mild-395 steel but are unconservative for the tested AHSS materials in this study.

- After exposure to temperatures above 300°C-400°C, the tested AHSS materials exhibit some degree of permanent strength loss. The highest grades (MS-1030, MS-1200) have the lowest post-fire retention factors. Codes currently do not provide retention factors for post-fire properties.

- The elevated temperature testing method (steady state versus transient state) did not significantly influence the measured strength properties. The testing method did, however, influence the measured elastic modulus to some extent, with transient tests leading to lower values of modulus than steady-state tests when the temperature exceeds 300°C (MS steels) or 400°C (DP steels).

## 6. Acknowledgments

Support from the Hopkins Extreme Materials Institute (HEMI) through the HEMI Seed Grant awarded to Dr. Gernay is gratefully acknowledged.

## Reference

[1] R. Kuziak, R. Kawalla, S. Waengler, Advanced high strength steels for automotive industry, Arch. Civ. Mech. Eng. 8 (2008) 103–117.

[2] H. Foroughi, B.W. Schafer, Simulation of conventional cold-formed steel sections formed from advanced high strength steel (AHSS), in: Annu. Stab. Conf. Struct. Stab. Res. Counc., San Antonio, TX, 2017.

[3] X. Yan, Y. Xia, H.B. Blum, T. Gernay, Elevated temperature material properties of advanced high strength steel alloys, J. Constr. Steel Res. 174 (2020) 106299.

[4] R. Qureshi, S. Ni, N. Elhami Khorasani, R. Van Coile, D. Hopkin, T. Gernay, Probabilistic Models for Temperature-Dependent Strength of Steel and Concrete, J. Struct. Eng. (United States). 146 (2020) 1–18. https://doi.org/10.1061/(ASCE)ST.1943-541X.0002621.

[5] EN 1993-1-2, Eurocode 3: Design of Steel Structures - Part 1-2: General Rules – Structural Fire Design, European Committee for Standardization (CEN), Brussels, 2005.

[6] AISC 360-16, Specification for Structural Steel Buildings, Chicago, 2016.

[7] J.H. Lee, M. Mahendran, P. Makelainen, Prediction of mechanical properties of light gauge steels at elevated temperatures, J. Constr. Steel Res. 59 (2003) 1517–1532. https://doi.org/10.1016/S0143-974X(03)00087-7.

[8] J. Chen, B. Young, Experimental investigation of cold-formed steel material at elevated temperatures, Thin-Walled Struct. 45 (2007) 96–110. https://doi.org/10.1016/j.tws.2006.11.003.

[9] H.T. Li, B. Young, Material properties of cold-formed high strength steel at elevated temperatures, Thin-Walled Struct. 115 (2017) 289–299. https://doi.org/10.1016/j.tws.2017.02.019.

[10] S. Gunalan, M. Mahendran, Experimental investigation of post-fire mechanical properties of cold-formed steels, Thin-Walled Struct. 84 (2014) 241–254. https://doi.org/10.1016/j.tws.2014.06.010.

[11] H.T. Li, B. Young, Residual mechanical properties of high strength steels after exposure to fire, J. Constr. Steel Res. 148 (2018) 562–571. https://doi.org/10.1016/j.jcsr.2018.05.028.

[12] W. Chen, J. Ye, J. Peng, B. Liu, Experimental Investigation of Postfire Mechanical Properties of Q345 and G550 Cold-Formed Steel, J. Mater. Civ. Eng. 31 (2019) 1–13. https://doi.org/10.1061/(ASCE)MT.1943-5533.0002791.

[13] X. Yan, Y. Xia, H.B. Blum, T. Gernay, Post-fire

mechanical properties of advanced high-strength cold-formed steel alloys, (Under review).
[14] ASTM E21, Standard Test Methods for Elevated Temperature Tension Tests of Metallic Materials, American Society for Testing and Materials, West Conshohocken, USA, 2009.
[15] ASTM E8/ E8M-16, Standard Test Methods for Tension Testing of Metallic Materials, ASTM International, West Conshohocken, PA, 2016.